AIP Advances

Effects of stress on the optical properties of epitaxial Nd-doped Sr0.5Ba0.5Nb2O6 films

Y. B. Yao, W. C. Liu, C. L. Mak, and K. H. Wong

Citation: AIP Advances **1**, 032172 (2011); doi: 10.1063/1.3647516
View online: http://dx.doi.org/10.1063/1.3647516
View Table of Contents: http://aipadvances.aip.org/resource/1/AAIDBI/v1/i3
Published by the American Institute of Physics.

Related Articles

Polycrystalline iron nitride films fabricated by reactive facing-target sputtering: Structure, magnetic and electrical transport properties
J. Appl. Phys. 110, 053911 (2011)

Phase-stabilization and substrate effects on nucleation and growth of (Ti,V)n+1GeCn thin films
J. Appl. Phys. 110, 053516 (2011)

Growth of a crystalline and ultrathin MgO film on Fe(001)
AIP Advances 1, 032156 (2011)

Structural and magnetic properties of quaternary Co2Mn1-xCrxSi Heusler alloy thin films
J. Appl. Phys. 110, 053903 (2011)

Texture and microstructure evolution in single-phase TixTa1xN alloys of rocksalt structure
J. Appl. Phys. 110, 043535 (2011)

Additional information on AIP Advances

Journal Homepage: http://aipadvances.aip.org
Journal Information: http://aipadvances.aip.org/about/journal
Top downloads: http://aipadvances.aip.org/most_downloaded
Information for Authors: http://aipadvances.aip.org/authors

ADVERTISEMENT

NEW!

iPeerReview
AIP's Newest App

Authors...
Reviewers...
Check the status of submitted papers remotely!

AIP | Publishing

Downloaded 06 Oct 2011 to 158.132.183.20. All article content, except where otherwise noted, is licensed under a Creative Commons Attribution 3.0 Unported license.
See: http://creativecommons.org/licenses/by/3.0/

Effects of stress on the optical properties of epitaxial Nd-doped $Sr_{0.5}Ba_{0.5}Nb_2O_6$ films

Y. B. Yao,[1] W. C. Liu,[1,2] C. L. Mak,[1,a] and K. H. Wong[1]
[1]*Department of Applied Physics, The Hong Kong Polytechnic University, Hong Hum, Kowloon, Hong Kong SAR, China*
[2]*National Laboratory of Solid State Microstructures and School of Modern Engineering and Applied Sciences, Nanjing University, Nanjing 210093, China*

(Received 18 July 2011; accepted 13 September 2011; published online 26 September 2011)

Nd-doped $Sr_{0.5}Ba_{0.5}Nb_2O_6$ (SBN) thin films with thicknesses ranging from 15 nm to 460 nm were grown on MgO (100) substrates using pulsed laser deposition technique. X-ray diffraction studies showed that the films were highly (001)-oriented and epitaxially grown on the substrates. Raman spectroscopy revealed the presence of residual stresses in the films especially for those with thicknesses below 100 nm. Transmittance and photoluminescence spectra revealed that the band-gap energies as well as the light-induced emission bands were shifted to higher energies as the film thickness decreased. The Nd^{3+} emission lines in the films were also dependent on film thickness. Origins of these observations were discussed based upon the stress as well as grain size effects. *Copyright 2011 Author(s). This article is distributed under a Creative Commons Attribution 3.0 Unported License*. [doi:10.1063/1.3647516]

I. INTRODUCTION

For miniaturization of devices, it is desired to fabricate thin film devices as thin as possible. Therefore, effects of film thickness on its properties are crucial issue in dealing with thin film devices. Stress and/or strain induced in thin films will definitely affect the macroscopic properties of the films.[1–3] For example, in-plane compressive stress in $PbTiO_3$ thin films induced an upshift of the Curie temperature[4] as well as an increase in dielectric constants.[2] Stresses in thin films usually are arisen from: 1) lattice constant mismatch; 2) impurities, defects and dislocations (resulted in inhomogeneous stress); 3) grain growth; and 4) difference in thermal expansion coefficients of the substrate and the film.[3,5–7] Stresses arisen from the last two sources can be greatly suppressed by employing a post-annealing process at low cooling rate.[6,7] Stresses in thin films have been determined nondestructively by Raman spectroscopy.[3,5–9] Pressure dependent Raman spectra has been studied in lead-base ferroelectrics, such as $PbTiO_3$ and $Pb(Zr_xTi_{1-x})O_3$ crystals.[10–12] The stresses in thin films were then estimated by comparing the Raman profiles of thin films with the pressure-dependent Raman spectra of the corresponding bulk samples.[1–5,8] Apart from lead-base ferroelectric thin films, few studies have been devoted to the investigation of stresses in other ferroelectric thin films using Raman spectroscopy. $Sr_{0.5}Ba_{0.5}Nb_2O_6$ (SBN), with a tetragonal tungsten-bronze (TTB) structure, is an important lead-free relaxor ferroelectric material in the area of photonics. The physics involved in this relaxor ferroelectric thin film is interesting especially when the thickness is below its threshold. In this paper, the correlation between film thickness and induced stress in epitaxial Nd-doped SBN thin films were studied by micro-Raman spectroscopy.

Besides stress, other optical properties of ferroelectric materials are also sensitive to grain size. For example, the band-gap energies increase with decreasing particle size or film thickness.[13,14] On the other hand, light-induced visible emission band increases in energy as the grain size decreases, as revealed by photoluminescence (PL) measurements in $BaTiO_3$,[15] $SrTiO_3$[15,16] and SBN

[a]corresponding author email: apaclmak@polyu.edu.hk

 © Author(s) 2011

Downloaded 06 Oct 2011 to 158.132.183.20. All article content, except where otherwise noted, is licensed under a Creative Commons Attribution 3.0 Unported license.
See: http://creativecommons.org/licenses/by/3.0/

nanocrystallines.[13] However, less attention has been paid to the effects of film thickness on the luminescence properties of rare-earth (RE) doped ferroelectric films. In current study, spectral properties of Nd-doped SBN thin films with different thicknesses were investigated by PL measurements. Our results showed that film thickness considerably influences the luminescence properties of the Nd^{3+} ions.

II. EXPERIMENTAL

Nd-doped SBN thin films were grown on MgO (100) substrates using pulsed laser deposition (PLD). The Nd-doped (3 mol%) SBN ceramic target was prepared by a conventional solid-state reaction method. Details of the target preparation process were given elsewhere.[17] For thin film preparation, a KrF excimer laser (Lambda Physik COMPex205, 248 nm, 20 ns) was used. Laser energy density of 4 J/cm^2, pulsed laser repetition rate of 5 Hz, oxygen pressure of 200 mTorr ($\sim$ 26 Pa), substrate temperature of 700°C and distance from target to substrate of 4 cm were employed during the deposition process. After the deposition, the films underwent in-situ annealing at 700°C for 15 min to improve their crystallinity. The film thickness was controlled through adopting different deposition durations (1 min, 2 min, 5 min, 10 min, 20 min and 30 min). The samples were denoted as S1, S2, S5, S10, S20 and S30, respectively, according to their deposition time.

The crystal structure of the annealed films was characterized by a four-circle X-ray diffractometer (XRD, Philips, X'pert) with Cu K_α radiation. The thickness of the film was measured directly from the cross-section micrograph obtained by a field emission scanning electron microscope (FE-SEM, JEOL JSM-6335F). The thicknesses of the samples S1, S2, S5, S10, S20 and S30 were determined to be 15 nm, 31 nm, 77 nm, 153 nm, 307 nm and 460 nm, respectively. Raman spectra were measured using 488 nm laser line of an air cooled Ar-ion laser. A microscope was used to focus the incident laser beam to a spot of about 100 μm in diameter. Room temperature Raman spectra were recorded by a 100x lens system in backscattering geometry using a Horiba-JobinYvon HR800 spectrometer equipped with a charge-coupled device detector. The optical transmittance measurements were accomplished using a two-beam spectrophotometer (Shimadzu UV-2101). The optical band-gap energies of the films were calculated based on the transmission data. For the PL measurements which were carried out at 12 K, a UV laser operating at 325 nm was used. Details of the PL setup were given elsewhere.[13]

III. RESULTS AND DISCUSSION

A. X-ray diffraction

Figure 1(a) shows the θ-2θ XRD patterns of the Nd-doped SBN thin films of different thicknesses. All the samples possessed a highly *c*-axis oriented texture. Using the Bragg diffraction equation, the *c*-lattice constants were determined to be 3.97 Å, which is slightly larger than that of the bulk sample (3.94 Å).[17] The full-width at half-maximum (FWHM) values of the (002) peaks were 0.40°, 0.38°, 0.31°, 0.36°, 0.28° and 0.26°, for samples S1 $\sim$ S30 respectively. The average crystallites sizes of the films were calculated from the (002) diffraction peak using the Scherrer equation:[18]

$$D = \frac{k\lambda}{\beta \cos\theta} \tag{1}$$

Here, k is a constant and equals to 0.89, β is the FWHM of the diffraction peak, λ is the x-ray wavelength and θ is the Bragg angle. The crystallites sizes D were estimated to be 21 nm, 23 nm, 27 nm, 25 nm, 30 nm and 33 nm for sample S1 to sample S30, respectively. As expected, the crystalline size slightly increased with the film thickness.

In order to evaluate the orientation properties of the films, XRD ω-scan (rocking curve) and phi-scan measurements were performed. Figure 1(b) shows the rocking curves of samples S1, S5 and S30. In general, the curves (except samples S20 and S30) were deconvoluted into two Gaussian profiles, one was very narrow while the other was very broad (as shown in samples S1 and S5).

Downloaded 06 Oct 2011 to 158.132.183.20. All article content, except where otherwise noted, is licensed under a Creative Commons Attribution 3.0 Unported license.
See: http://creativecommons.org/licenses/by/3.0/

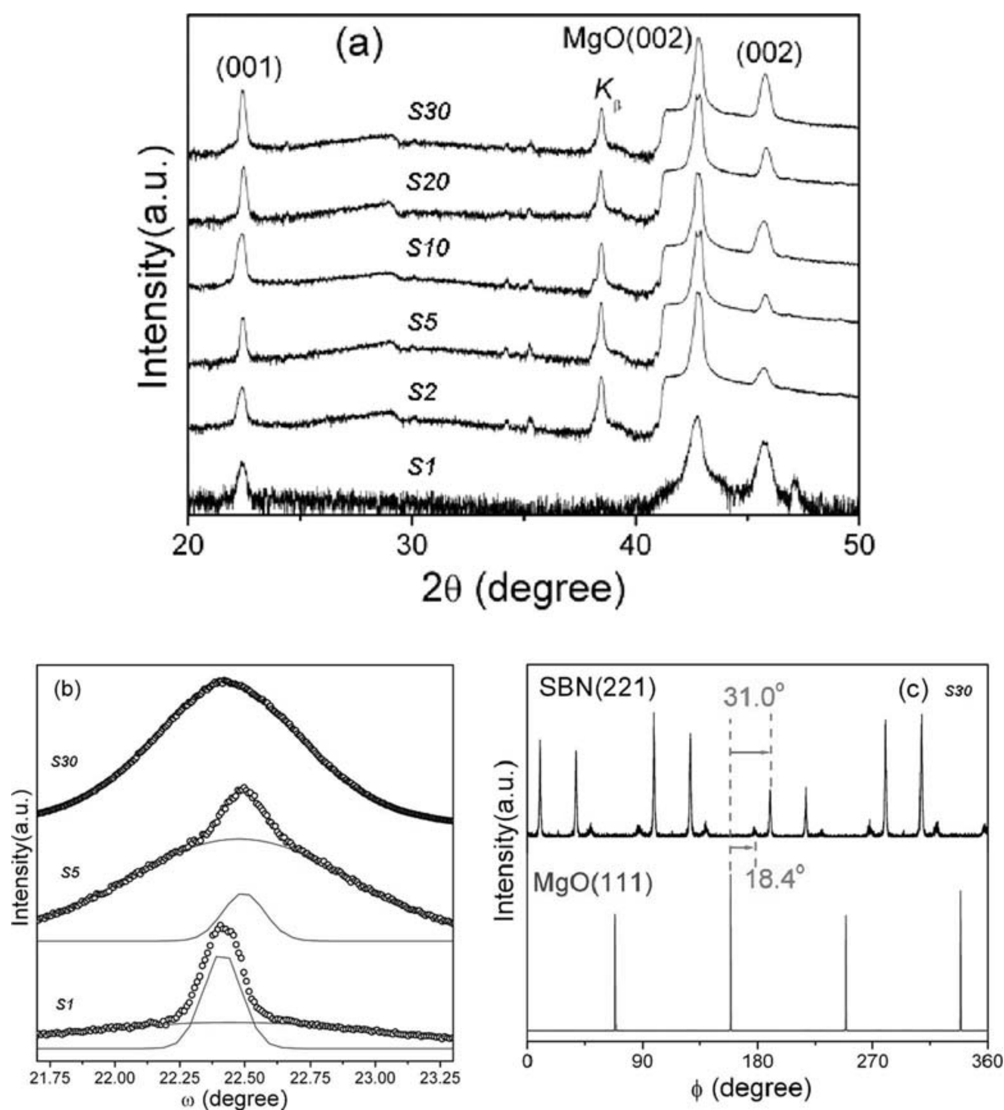

FIG. 1. XRD (a) θ-2 θ scan, (b) ω-scan (rocking curves) patterns of Nd-doped SBN films with different thickness, and (c) φ-scan pattern of sample S30.

The relative intensity of the narrow peak to the broad peak decreased with increased film thickness. For samples S20 and S30, the narrow peaks seemed to be disappeared eventually with only the broad profile remained. The FWHMs of the broad profiles for samples S1 to S30 were 1.33°, 1.15°, 1.10°, 1.18°, 1.14° and 0.97°; while the FWHMs of the narrow profiles (sample S1 to sample S10) were 0.15°, 0.35°, 0.20° and 0.23°, respectively. These XRD profiles suggested that two regions with different degrees of orientation existed in the films. The narrow profile represented a highly oriented interfacial region close to the substrate while the broad peak stood for a distorted region far from the substrate. Similar observation was also reported in expitaxial $SrBi_2Ta_2O_9$ and $SrBi_2Nb_2O_9$ films grown on $SrTiO_3$.[19] Figure 1(c) shows the Phi-scan of sample S30. Similar phi-scan results were also found in other samples. In fig. 1(c), two sets of anti-phase domains were observed. One set is rotated at ±18.4° along the c-axis and the other is rotated at ±31.0°. These in-plane relationships have been observed by other researchers.[20–22] Minimization of the lattice mismatch as well as electrostatic energy in the interface area between the film and the substrate governs such in-plane orientations.[20–22] The lattice mismatch of these two kinds of in-plane orientations were 1.5% (±18.4°) and -6.4% (±31.0°), respectively.[20] On the basis of our XRD results, we believed that our films are well-crystallized and epitaxially grown on the MgO substrates.

Downloaded 06 Oct 2011 to 158.132.183.20. All article content, except where otherwise noted, is licensed under a Creative Commons Attribution 3.0 Unported license.
See: http://creativecommons.org/licenses/by/3.0/

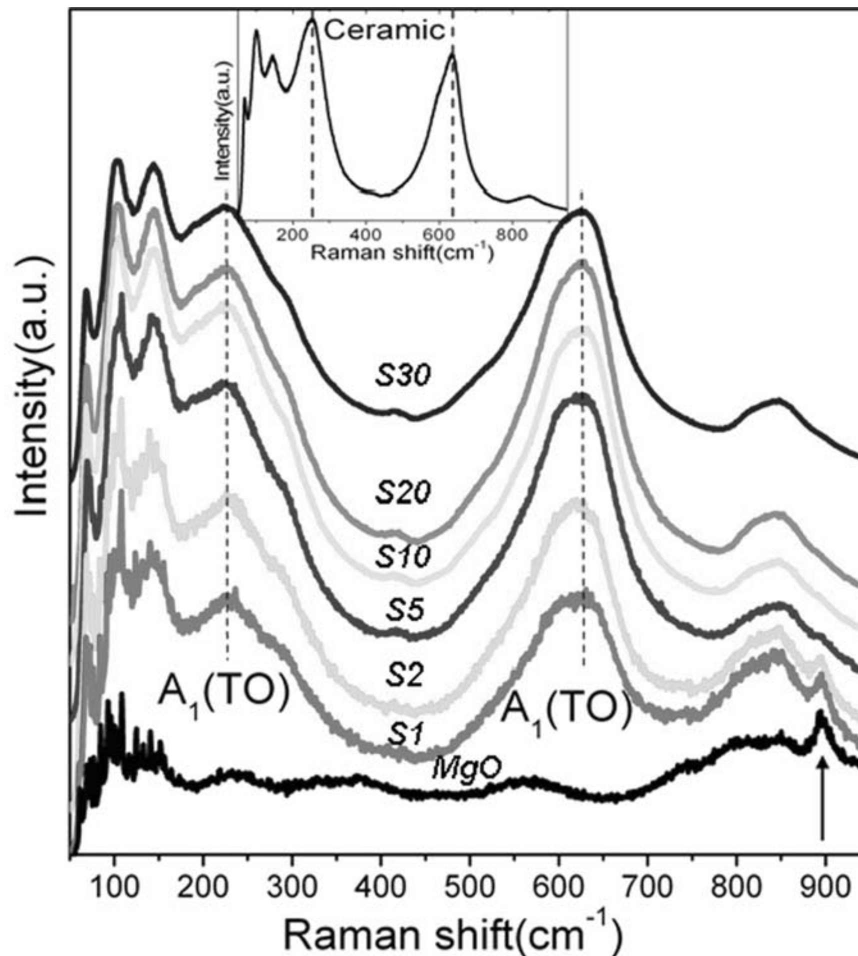

FIG. 2. Raman spectra of Nd-doped SBN films of different thickness measured at room temperature. Inset shows the Raman spectrum of Nd-doped SBN ceramic sample.

B. Stresses in the films evaluated by micro-Raman spectroscopy

Raman spectra of films of different thicknesses are shown in Fig. 2. Inset of the figure shows the Raman spectrum of the bulk ceramic target for comparison. In general, the Raman profiles of the films were similar to that of the bulk sample. As expected, the intensity of the spectra increased with film thickness due to an increase of scattering volume. The Raman peak at 893 cm^{-1}, indicated by the arrow in Fig. 2 and originated from the substrate, disappeared for films of thicknesses ≥ 153 nm. Two dominant A_1 transverse optical modes around 625 cm^{-1} and 225 cm^{-1} were clearly identified in the spectra. They were assigned as the Nb-O stretching and O-Nb-O bending modes of the internal vibrations of NbO_6 octahedra, respectively.[23–26] These two A_1(TO) bands were both deconvoluted into two subpeaks, as shown in Fig. 3(a) and 3(b). For the 625 cm^{-1} mode, the high frequency peak was located around 642 cm^{-1} and its peak position was independent of film thickness; while the low frequency subpeak decreased from 610 cm^{-1} to 601 cm^{-1} as the film thickness increased from 15 nm to 460 nm. On the other hand, for the 225 cm^{-1} band, the high frequency subpeak increased from 283 cm^{-1} to 293 cm^{-1} as thickness increased from 15 nm to 460 nm, while the low frequency subpeak was invariant at 228 cm^{-1} for all the films. Summary of the positions as well as the FWHMs of the thickness-sensitive subpeaks around 605 cm^{-1} and 290 cm^{-1} were illustrated in Fig. 3(c) and 3(d), respectively. For both subpeaks, the FWHM decreased rapidly with film thickness, especially when the film thickness was below 100 nm, and then it became almost constant. The peak position of the subpeak around 605 cm^{-1} exhibited a similar trend with the FWHM, while the peak position of the

Downloaded 06 Oct 2011 to 158.132.183.20. All article content, except where otherwise noted, is licensed under a Creative Commons Attribution 3.0 Unported license.
See: http://creativecommons.org/licenses/by/3.0/

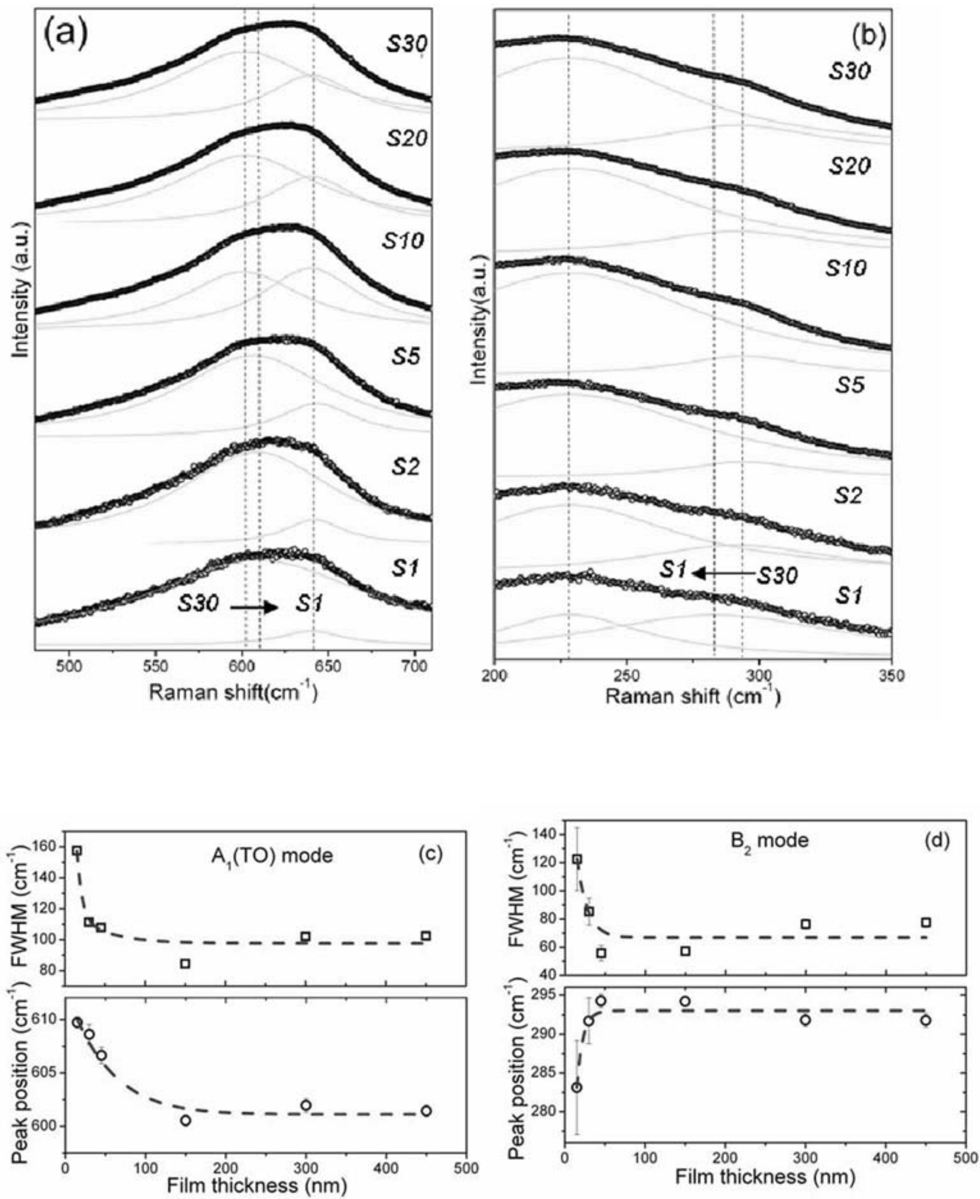

FIG. 3. Enlarged views of (a) 620 cm^{-1}and (b) 250 cm^{-1} Raman bands of Nd-doped SBN films of different thicknesses. (c) and (d) show the FWHMs and band peak positions of the deconvoluted subpeaks at 605 cm^{-1} and 290 cm^{-1}, respectively.

subpeak around 290 cm^{-1} showed an opposite trend. It increased rapidly when the film thickness was below 100 nm and then kept almost constant. This discrepancy might be due to the different origin of these two subpeaks. The 605 cm^{-1} subpeak belongs to an A_1(TO) mode and the corresponding bulk value was 596 cm^{-1}.[23] The 290 cm^{-1} subpeak was not clearly observed in our bulk sample. It was assigned as the B_2 mode in published SBN Raman data[23–26] and the corresponding bulk value was around 304 cm^{-1} (SBN crystal).[24] It is noticed that when the film thickness increased above 100 nm, the positions of these two modes in our thin film samples approached to those of the bulk values.

For PZT films grown on MgO substrate, Lappalainen *et al*. observed an abrupt decrease in the frequencies of both $A_1(TO_2)$ and $E(TO_2)$ modes as film thickness decreased below 150 nm.[3] A large compressive stress in these films was responsible for the frequency decrease of the Raman modes. Xu *et al*. found that the in bulk PZT sample, the frequency of $A_1(TO_3)$ mode increased while the $E(LO_3)$

Downloaded 06 Oct 2011 to 158.132.183.20. All article content, except where otherwise noted, is licensed under a Creative Commons Attribution 3.0 Unported license.
See: http://creativecommons.org/licenses/by/3.0/

mode decreased because of an external bending stress.[8] Thus, it is believed that the applied stress will either increase or decrease the Raman modes, depending on the symmetry of the Raman modes. In current case, the induced stress in the films might be responsible for the increase of the frequency of the A_1(TO) mode as well as the decrease of the frequency of the B_2 mode. Unfortunately, the situations herein were more complicated as compared with those in PZT films.[3,8] Firstly, two kinds of stresses (in-plane compressive and tensile) were present in our SBN thin films which were originated from different in-plane orientations with respect to the substrate ($\pm 31.0^\circ$ and $\pm 18.4^\circ$, respectively). Secondly, the crystal structure of SBN ('unfilled' tetragonal tungsten bronze)[17] is more disordered as compared to that of the PZT (pseudo-cubic).[3,8] This disorder structure also affects the positions as well as the FWHMs of the Raman modes. In order to fully understand the relationship between the specific Raman modes and the stresses in our films, pressure-dependent Raman spectroscopic studies of the SBN crystal should be performed in order to reveal the physics.

C. Band-gap energy and PL properties

The transmittance spectra of samples S1 to S30 are shown in Fig. 4(a). All samples showed transmittance over 80% in the wavelength range between 400 nm and 900 nm. Well-defined interference fringes appeared in thick samples (S10 ∼ S30). The well structured and smooth oscillations of the transmittance profiles indicate that the films have flat surfaces and uniform thickness. The absorption coefficients α of the sample near the absorption edge were obtained from the transmittance:[27]

$$\alpha = \frac{1}{d}\ln\left(\frac{1}{T}\right), \tag{2}$$

where α, d, and T are absorption coefficient, film thickness and transmittance, respectively. By plotting $(\alpha h\nu)^2$ vs. $h\nu$, the optical band-gaps (E_g) of the samples were realized as the intercepts with x-axis,[27] as shown in Fig. 4(b). For samples S1 ∼ S30, the band-gap energies were found to be 4.48, 4.38, 4.11, 3.96, 3.89, and 3.86 eV, respectively. The E_g of SBN single crystal is reported to be 3.4 eV,[23] which is much smaller than those of the films. As shown in inset of Fig. 4(b), the E_g increased with decreasing thickness, especially when the film thicknesses were below 100 nm (samples S1 ∼ S5). Similar phenomenon has also been observed in $BaTiO_3$[1] and $SrTiO_3$[14] thin films. Zhu *et al.* attributed the increase of E_g with decreasing thickness to the increase of lattice constant, tensile stress, and lattice distortion with decreasing film thickness.[1] Bao *et al.* found that thinner films contained more amorphous phase and smaller crystallites.[14] Thus, the quantum-size effect in the thinner film induced a dramatic increase in the band-gap energy.[13–16] In the present case, the grain size increased while the residual stress reduced with an increase in the film thickness, as confirmed by our XRD and Raman results. Therefore, we believe that the decrease of E_g with the increase of the film thickness is related with the increase of grain size as well as the decrease of residual stress.

The PL spectra of samples S1 to S30 as well as pure MgO substrate are shown in Fig. 5(a). For all the films, a strong emission band centered at 390 nm (denoted as '①') and a weak and broad shoulder around 500 ∼ 600 nm (2.48 ∼ 2.07 eV, marked as '③') were observed. On the other hand, the MgO substrate exhibited a strong and broad peak at ∼ 450 nm (indicated as '②'), which was related to oxygen vacancies.[28] As shown in Fig. 4(a), the films are transparent to the emission light from the substrate (∼ 450 nm). Thus, the observed PL spectra included signals from the MgO substrate. In order to clearly show the PL profiles from the films alone, the films' spectra were subtracted by that of the MgO substrate. Figure 5(b) shows the spectra after the subtraction. The PL spectrum of the corresponding ceramic target was also shown for comparison. In the ceramic sample, a strong peak centered at 603 nm and a very weak 390 nm peak (2.06 eV) were observed. The strong band is previously assigned as the radiative recombination of electron-hole polarons in the charge transfer vibronic exitons (CTVEs).[29,30] The strong and narrow band ('①' in Fig. 5(a)) at ∼ 390 nm (3.18eV) appeared to be irrespective of the film thickness. The relative intensity of this band increased significantly in the films, as compared with the ceramic sample. This might be due to the resonance effect with the similar emission band from the MgO substrate. Similar effects were also observed in SBN nanoparticles embedded in silica matrix.[13] Thickness dependence of the host

Downloaded 06 Oct 2011 to 158.132.183.20. All article content, except where otherwise noted, is licensed under a Creative Commons Attribution 3.0 Unported license.
See: http://creativecommons.org/licenses/by/3.0/

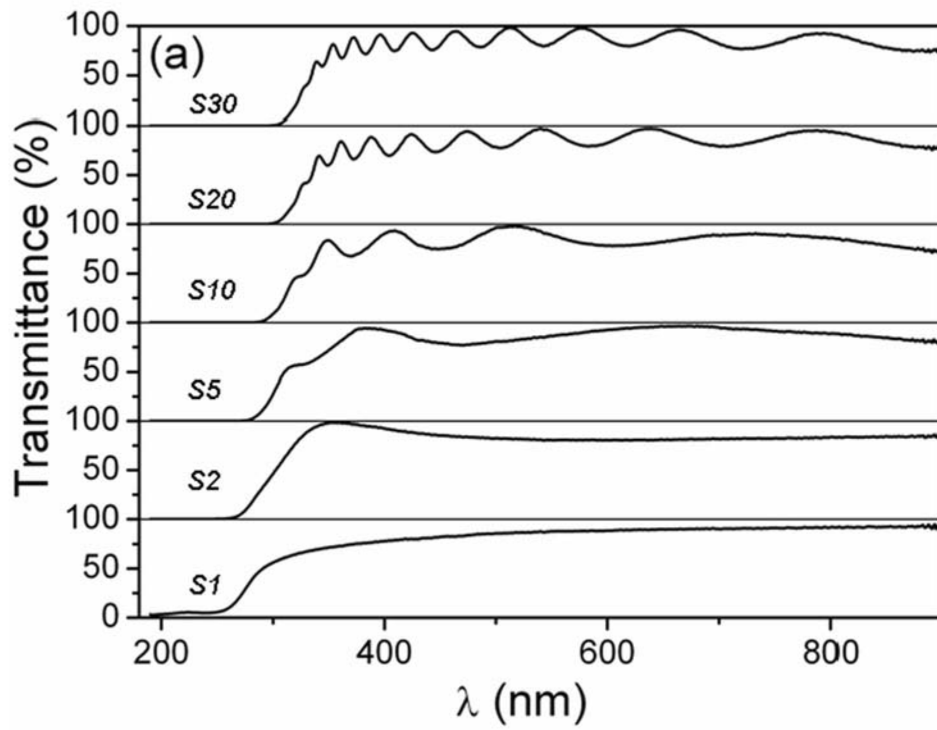

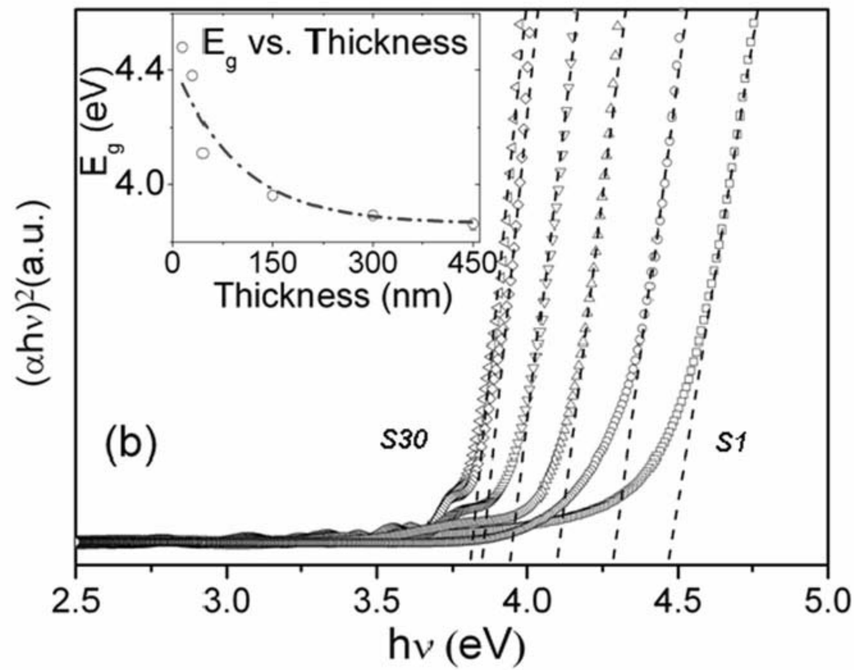

FIG. 4. (a) Transmittance spectra and (b) plots of $(\alpha h\nu)^2$ vs. $h\nu$ of Nd-doped SBN films with different thicknesses. Inset in (b) shows the thickness dependence of the calculated band-gap energy (E_g).

Downloaded 06 Oct 2011 to 158.132.183.20. All article content, except where otherwise noted, is licensed under a Creative Commons Attribution 3.0 Unported license.
See: http://creativecommons.org/licenses/by/3.0/

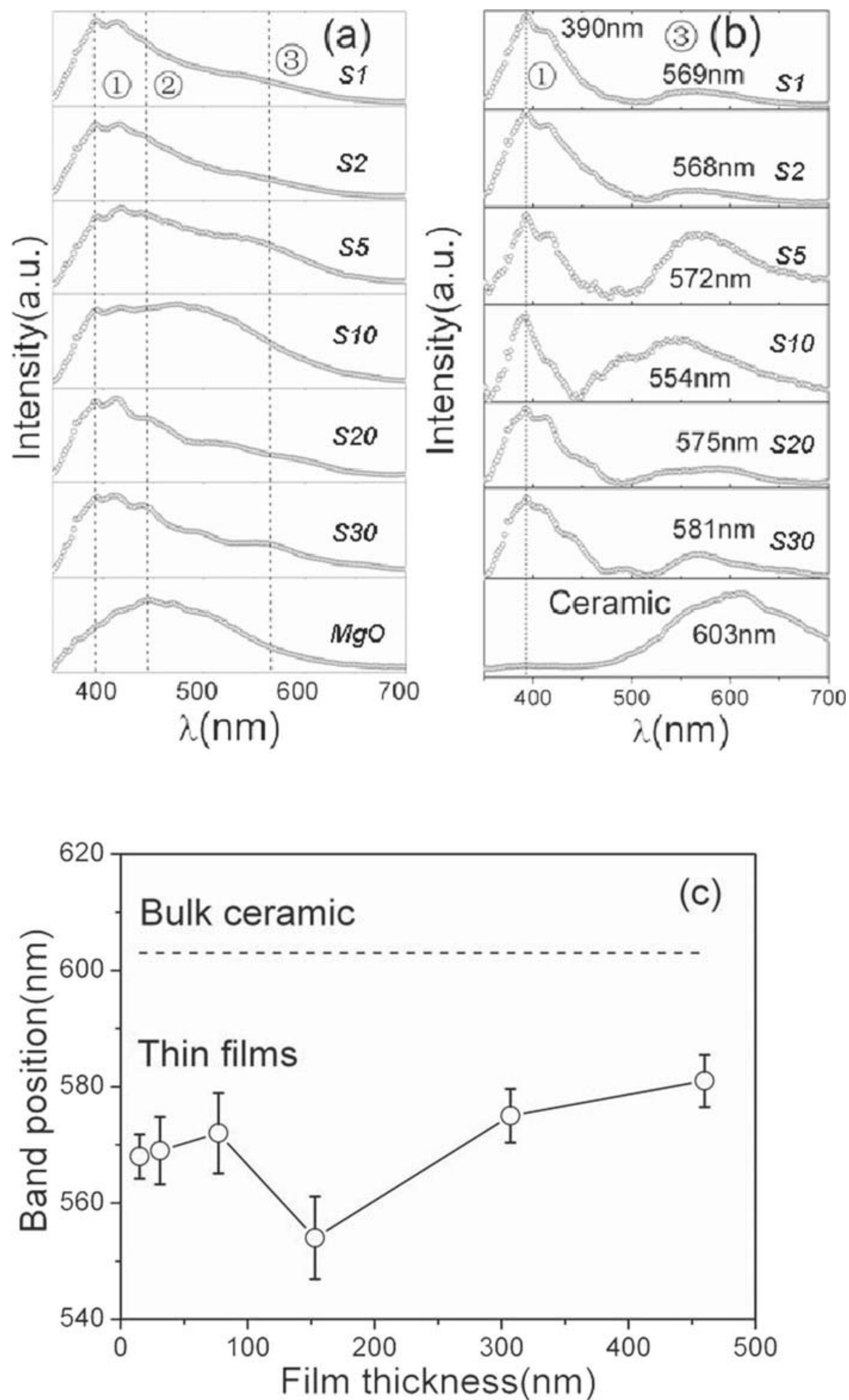

FIG. 5. (a) PL spectra of MgO substrate and the Nd-doped SBN thin films with different thicknesses measured by a laser source at 325 nm and at a temperature of 12K; (b) the spectra after subtracting the films' PL spectra by that of the MgO substrate. The PL spectra of the corresponding ceramic sample is also included in (b) for comparison; (c) Thickness dependence of the host SBN emission band.

Downloaded 06 Oct 2011 to 158.132.183.20. All article content, except where otherwise noted, is licensed under a Creative Commons Attribution 3.0 Unported license.
See: http://creativecommons.org/licenses/by/3.0/

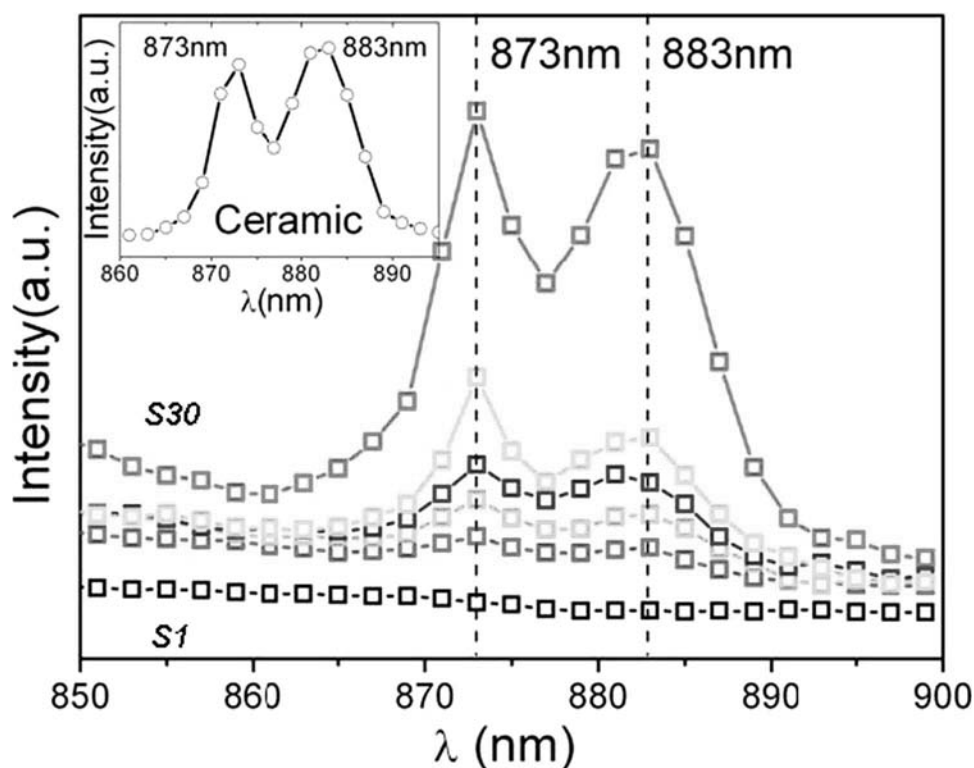

FIG. 6. Thickness dependence of the Nd^{3+} characteristic emission lines. Inset shows the Nd^{3+} emission lines in bulk ceramic sample.

emission band ('③' in Fig.5(b)) is illustrated in Fig. 5(c). General speaking, the peak position of this band increased with film thickness. This might be due to the decrease of residual stress with the increase in film thickness.

Apart from the emission band from SBN, the Nd^{3+} ions characteristic emission lines at 873 nm and 883 nm ($^4F_{3/2} \rightarrow {}^4I_{9/2}$ transition)[31] were also observed in thick samples (samples S5 ∼ S30), as shown in Fig. 6. The positions of these lines were exactly the same as those in the bulk ceramics and seemed to be independent from film thickness. However, the emission intensity decreased while the width increased as the film thickness decreased. This might be due to the fact that as the film thickness decreased the sample scattering volume decreased and internal stress increased (as shown in the Raman scattering results). These two factors might be responsible for the reduction of peak intensity and finally no Nd^{3+} emission lines were observed in the films with thickness $\leq$ 30nm. Similar results of stress dependence of PL spectra in RE-doped SBN were reported by Liu *et al.*[32] They found that the emission from Pr^{3+} in SBN thin film became much stronger after the film was annealed at a high temperature (1000°C) and for a long annealing time (10 hours). This was attributed to the release of residual stress in the film after annealing, indicating that stress could weaken the PL emissions of RE ions. On the other hand, in Nd^{3+} doped $LiNbO_3$ material, the Nd^{3+} emission lines in thin film form were much broader than those in single crystal form, which was believed to be caused by the stresses and lattice imperfections in thin films.[33] Therefore, the observed increase of Nd^{3+} linewidth with decreasing thickness in our SBN films is related with the increase of the stress.

IV. CONCLUSIONS

In summary, we systematically studied the effects of stress on the Raman and luminescence properties of PLD derived epitaxial Nd-doped SBN thin films when the thicknesses are varied from 15 nm to 460 nm. Thickness dependence of stress in the films was revealed by Raman spectroscopy.

Downloaded 06 Oct 2011 to 158.132.183.20. All article content, except where otherwise noted, is licensed under a Creative Commons Attribution 3.0 Unported license.
See: http://creativecommons.org/licenses/by/3.0/

It was found that the stress increased as the film thickness decreased, especially as the thickness below 100 nm. The band-gap energies were found to be increased greatly as the film thickness decreased below 100 nm. From low temperature PL measurements, it was found that the SBN host emission band showed dependence on the film thickness, while the position of the Nd^{3+} emission lines were found to be independent on the film thickness.

ACKNOWLEDGMENT

This work was supported by a research grant of The Hong Kong Polytechnic University (GYH08).

[1] J. S. Zhu, X. M. Lu, W. Jiang, W. Tian, M. Zhu, M. S. Zhang, X. B. Chen, X. Liu and Y. N. Wang, J. Appl. Phys. **81**, 1392 (1997).
[2] D. S. Fu, T. Ogawa, H. Suzuki and K. Ishikawa, Appl. Phys. Lett. **77**, 1532 (2000).
[3] J. Lappalainen, V. Lantto, J. Frantti and J. Hiltunen, Appl. Phys. Lett., **88**, 252901 (2006).
[4] G. A. Rossetti Jr., L. E. Cross and K. Kushida, Appl. Phys. Lett., **59**, 2524 (1991).
[5] B. Dkhil, E. Defaÿ and J. Guillan, Appl. Phys. Lett. **90**, 022908 (2007).
[6] J. Zhu, S. K. Singh, P. A. Thomas and S. B. Palmer, Cryst. Res. Technol. **34**, 1205 (1999).
[7] L. B. Freund and S. Suresh, Thin Film Materials: Stress, *Defect Formation and Surface Evolution*, Cambridge University Press, Cambridge, 2003.
[8] W. H. Xu, D. Lu and T. Y. Zhang, Appl. Phys. Lett. **79**, 4112 (2001).
[9] M. Leoni, U. Welzel, P. Lamparter, E. J. Mittemeijer and J. D. Kamminga, Philos. Mag. A. **81**, 597 (2001).
[10] J. A. Sanjurjo and E. López-Cruz, Phys. Rev. B **28**, 7260 (1983).
[11] M. Deluca, T. Sakashita, W. Zhu, H. Chazono and G. Pezzotti, J. Appl. Phys. **101**, 083526 (2007).
[12] J. Kreisel and P. Bouvier, J. Raman Spectrosc. **34**, 524 (2003).
[13] S. G. Lu, C. L. Mak and K. H. Wong, J. Appl. Phys., **94**, 3422 (2003).
[14] D. H. Bao, X. Yao, N. Wakiya, K. Shinozaki and N. Mizutani, Appl. Phys. Lett. **79**, 3767 (2001).
[15] J. Meng, Y. Huang, W. Zhang, Z. Du, Z. Zhu and G. Zou, Phys. Lett. A **205**, 72 (1995).
[16] W. F. Zhang, Z. Yin, M. S. Zhang, Z. L. Du, and W. C. Chen, J. Phys.: Condes. Matte **11**, 5655 (1999).
[17] Y. B Yao, C. L. Mak, K. H. Wong, S. G. Lu and Z. K. Xu, Int. J. Appl. Ceram. Technol. **6**. 671 (2009).
[18] W. C. Liu, D. Wu, A. D. Li, H. Q. Ling, Y. F. Tang, N. B. Ming, Appl. Surf. Sci. **191**, 181 (2002).
[19] S. M. Zanetti, E. R. Leite, E. Longo and J. A. Varela, Mater. Res. **4**, 157 (2001).
[20] C. M. Rouleau, G. E. Jellison, Jr. and D. B. Beach, Appl. Phys. Lett. **82**, 2990 (2003).
[21] S. Schwyn Thöny, K. E. Youden, J. S. Harris, Jr. and L. Hesselink, Appl. Phys. Lett. **65**, 2018 (1994).
[22] P. R. Willmott, R. Herger, B. D. Patterson and R. Windiks, Phys. Rev. B **71**, 144114 (2005).
[23] C. David, A. Tunyagi, K. Betzler and M. Wöhlecke, Phys.Stat.Sol. (b) **244**, 2127 (2007).
[24] E. Amzallag, T. S. Chang, R. H. Pantell and R. S. Feigelson, J. Appl. Phys. **42**, 3254 (1971).
[25] R. E. Wilde, J. Raman Spectrosc. **22**, 321 (1991).
[26] H. R. Xia, K. X. Wang, B. Y. Zhao, H. C. Chen, X. L. Lu, Q. Z. Jiang, P. J. Sun and L. J. Hu, Acta Phys. Sin. **45**, 232 (1996).
[27] W. C. Liu, C. L. Mak, K. H. Wong, D. Y. Wang and H. L. W. Chan, J. Appl. Phys., **100**, 033507 (2006).
[28] Y. Chen, J. L. Kolopus and W. A. Sibley, Phys. Rev. **186**, 865 (1969).
[29] V. S. Vikhnin, R. I. Eglitis, S. E. Kapphan, G. Borstel and E. A. Kotomin, Phys. Rev. B **65**, 104304 (2002).
[30] V. S. Vikhnin, S. Avanesyan, H. Liu and S. E. Kapphan, J. Phys. Chem. Solids **63**, 1677 (2002).
[31] J. J. Romero, D. Jaque, L. E. Bausá, A. A. Kaminskii and J. García Solé, J. Lumin. **87-89**, 877 (2000).
[32] H. Liu, O. Vasquez, V. R. Santiago, L. Díaz, F. E. Fernandez, L. Liu, L. Xu an F. Gan, J. Lumin. **108**, 37 (2004).
[33] J. E. Alfonso, M. J. Martín and C. Zaldo, Appl. Phys. Lett. **71**, 2904 (1997).

Downloaded 06 Oct 2011 to 158.132.183.20. All article content, except where otherwise noted, is licensed under a Creative Commons Attribution 3.0 Unported license.
See: http://creativecommons.org/licenses/by/3.0/